Clean Transfer of Wafer-Scale Graphene *via* Liquid Phase Removal of Polycyclic Aromatic Hydrocarbons

Hyun Ho Kim,[†] Boseok Kang,[†] Ji Won Suk,[‡,#] Nannan Li,[§] Kwang S. Kim,[⊥] Rodney S. Ruoff,[‡,▽] Wi Hyoung Lee,[*,∥] and Kilwon Cho[*,†]

[†]Department of Chemical Engineering, Pohang University of Science and Technology, Pohang 790-784, Korea, [‡]Department of Mechanical Engineering and the Materials Science and Engineering Program, The University of Texas at Austin, Austin, Texas 78712, United States, [§]Department of Physics, Pohang University of Science and Technology, Pohang 790-784, Korea, [⊥]Department of Chemistry, School of Natural Science, Ulsan National Institute of Science and Technology (UNIST), Ulsan 689-798, Korea, and [∥]Department of Organic and Nano System Engineering, Konkuk University, Seoul 143-701, Korea. [#]Present address: School of Mechanical Engineering, Sungkyunkwan University, Suwon 440—746, Korea. [▽]Present address: Institute of Basic Sciences Center for Multidimensional Carbon Materials and Department of Chemistry and School of Materials Science and Engineering, Ulsan National Institute of Science and Technology (UNIST), Ulsan 689—798, Korea.

ABSTRACT Pentacene ($C_{22}H_{14}$), a polycyclic aromatic hydrocarbon, was used as both supporting and sacrificing layers for the clean and doping-free graphene transfer. After successful transfer of graphene to a target substrate, the pentacene layer was physically removed from the graphene surface by using intercalating organic solvent. This solvent-mediated removal of pentacene from graphene surface was investigated by both theoretical calculation and experimental studies with various solvents. The uses of pentacene and appropriate intercalation solvent enabled graphene transfer without forming a residue from the supporting layer. Such residues tend to cause charged impurity scattering and unintentional graphene doping effects. As a result, this clean graphene exhibited extremely homogeneous surface potential profiles over a large area. A field-effect transistor fabricated using this graphene displayed a high hole (electron) mobility of 8050 $cm^2/V \cdot s$ (9940 $cm^2/V \cdot s$) with a nearly zero Dirac point voltage.

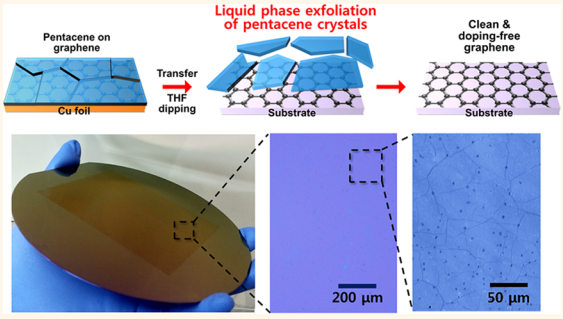

KEYWORDS: graphene · pentacene · chemical vapor deposition · transfer · graphene transistors

Graphene, a two-dimensional form of carbon, has attracted enormous research interest due to its excellent thermal,[1] mechanical,[2] optical,[3] and electrical properties.[4−13] Electrical measurements of monolayer graphene were first conducted using mechanically exfoliated samples from natural graphite;[14] Mechanical exfoliation tends to provide a low yield, the process is time-consuming, and sizes of the exfoliated graphene are limited to a few tens of micrometers. Researchers have developed methods for synthesizing large-area graphene, including a solution process that uses graphene oxide as a starting material,[15−17] thermal decomposition of SiC,[18] and chemical vapor deposition (CVD).[19−21] Among these methods, CVD offers the most promise for synthesizing high-quality large-area graphene; however, CVD requires that the graphene be transferred onto a target substrate.[6,22,23] Note that CVD-grown graphene is generally implemented on a catalytic metal substrate (*e.g.*, Cu,[19] Ni[24]). The effective transfer of CVD-grown monolayer graphene requires a supporting layer because monolayer graphene itself can be easily cracked during the etching of the catalytic substrate, commonly performed in a water-based etching solution (*e.g.*, $(NH_4)_2S_2O_8$, $Fe(NO_3)_3$). Organic coating layers, such as poly(methyl methacrylate) (PMMA), have conventionally been used as a supporting layer for graphene transfer because such layers are highly scratch/impact resistant and generally tough.[25] Additionally, these layers can be chemically dissolved[4,23,26] or thermally removed after transferring the graphene onto another substrate.[7,27] The use of PMMA as a supporting layer suffers from several disadvantages. Chemical dissolution processes using

* Address correspondence to whlee78@konkuk.ac.kr, kwcho@postech.ac.kr.

Received for review November 21, 2014 and accepted March 25, 2015.

Published online March 25, 2015
10.1021/nn5066556

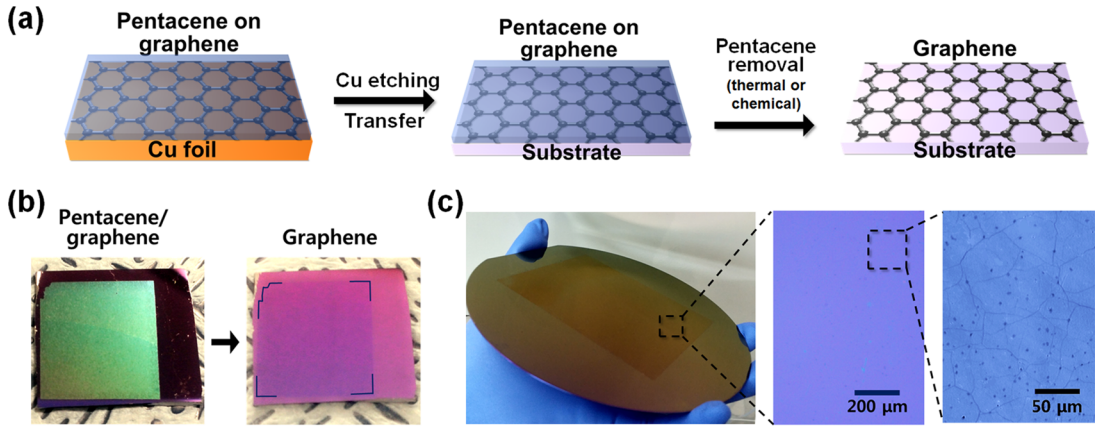

Figure 1. (a) Transfer procedure of graphene from a Cu foil to an arbitrary substrate using a pentacene supporting layer. (b) Photographs of pentacene/graphene and graphene before and after pentacene removal with THF. (c) Photographs of transferred graphene on 6-in. SiO_2/Si wafer and optical microscopy images (50×, 200×) of transferred graphene after chemical removal of pentacene layer.

organic solvents inevitably generate residue of polar PMMA on the graphene surface that trigger charged impurity scattering and unintentional graphene doping effects.[28] On the other hand, thermal removal processes cause substrate-induced graphene doping as a result of intimate interaction between the graphene and the substrate with H_2O and/or O_2 molecules.[29−31] Thus, a new supporting layer that could enable the clean and doping-free transfer of CVD-grown graphene is required. Meanwhile, a direct transfer method without supporting layer[22,32] has been recently developed by several research groups. Although their method clearly solved the issues of residue-free transfer, they did not achieve clean and doping-free graphene transfer onto arbitrary substrates.

Here, we describe the development of a method of providing the clean and doping-free transfer of large-area graphene onto arbitrary substrates through the use of a pentacene ($C_{22}H_{14}$) thin film supporting layer. Because charge transfer does not occur between pentacene and graphene, the band structure and Fermi level of graphene are not affected by the presence of the pentacene layer on the graphene surface.[33,34] After transferring the pentacene/graphene onto a target substrate, pentacene could be removed by thermal evaporation or chemical desorption using tetrahydrofuran (THF). Our results showed that unintentional substrate-induced doping occurred during the thermal removal of pentacene. On the other hand, chemical desorption of the pentacene produced undoped graphene without a pentacene residue as confirmed by atomic force microscopy (AFM) images, Raman spectra, and scanning kelvin probe force microscopy (KPFM) images. Finally, graphene field-effect transistors (GFETs) were prepared using a pentacene supporting layer. These GFETs showed a high field-effect mobility with a minimal shift in the Dirac point voltage (V_{Dirac}).

RESULTS AND DISCUSSION

The transfer method involving pentacene is schematically illustrated in Figure 1a. The 200 nm-thick pentacene was thermally evaporated onto CVD-grown graphene on a copper foil.[7] We found that a pentacene supporting layer with a thickness below 200 nm tends to be torn out during transfer process. Thus, 200 nm-thick pentacene was used as a supporting layer. The Cu foil was etched away using an aqueous ammonium persulfate ($(NH_4)_2S_2O_8$) solution and was rinsed with deionized water. The floated pentacene/graphene film as shown in Figure S1 was transferred onto a SiO_2 (285 nm)/Si wafer, and the pentacene was chemically removed by THF (or thermally removed). From the photographs (Figure 1b), it was confirmed that the pentacene supporting layer was selectively removed without peeling off the graphene from the SiO_2/Si substrate. In addition, optical microscopy images (50×, 200×) were obtained, and a photograph of successfully transferred graphene onto a 6-in. Si wafer was taken, as shown in Figure 1c. The optical microscopy image showed that the microsized cracks were not generated during transfer process.

Meanwhile, the pentacene layer deposited on graphene can also be thermally removed (250 °C for 1 h) after transfer. Optical microscopy images and field-emission scanning electron microscopy (FESEM) images (see Supporting Information, Figure S2) were obtained to analyze the transferred graphene. Although a large-area pentacene/graphene layer was found to be transferred without introducing notable cracks, there were pentacene residues on graphene surface.

The presence of a supporting layer residue has been shown to alter the surface and electrical properties of graphene.[28] The electrical properties of graphene are particularly sensitive to the presence of a residue. In this regard, the clean and crack-free transfer of large-area

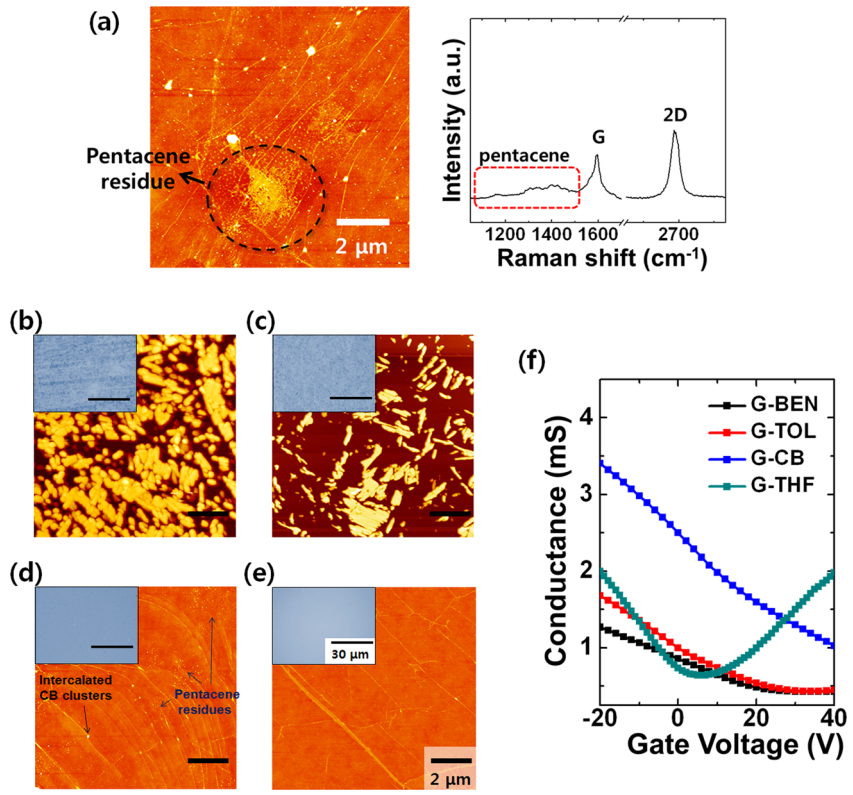

Figure 2. (a) AFM image and Raman spectrum of the transferred pentacene/graphene after thermal annealing (G-TR). AFM images and optical microscopy images (inset) of pentacene/graphene after dipping into (b) benzene (G-BEN), (c) toluene (G-TOL), (d) chlorobenzene (G-CB), and (e) tetrahydrofuran (G-THF). (f) Gate-dependent conductance of G-Ben, G-TOL, G-CB, and G-THF.

graphene is a prerequisite for the fabrication of high-performance graphene devices. The presence of a pentacene residue on graphene was confirmed by Raman spectroscope (Alpha 300R, WITec, λ = 532 nm) and atomic force microscope, as shown in Figure 2a. The graphene prepared by the thermal removal of pentacene (G-TR) displayed broad peaks ranging from 1100 to 1550 cm^{-1} in the normalized Raman spectrum. These peaks were attributed to the presence of physisorbed pentacene molecules, which display D_{2h} molecular symmetry bands at 1533, 1501, 1457, 1409, 1371, 1178, and 1158 cm^{-1}.[35] The AFM images of the graphene surface revealed the presence of sub-100 nm pentacene residues. These results clearly demonstrated that pentacene molecules present on the graphene surface were not completely removed during annealing at 250 °C for 1 h (under a vacuum). Increasing the annealing temperature to 300 °C, which is close to the sublimation temperature of pentacene, still produced a pentacene residue. The strong $\pi-\pi$ interactions between the pentacene molecules and graphene prohibited the complete desorption of the pentacene molecules from the graphene surface.

Intercalating molecules that weaken the $\pi-\pi$ interactions were thought to be necessary for the clean removal of pentacene. The thermal removal process was replaced with a chemical cleavage process involved in intercalating molecules between the pentacene supporting layer and graphene. To find a proper solvent, we performed experiments using various solvents. *N*-Methyl-2-pyrrolidone (NMP) has been used for liquid phase exfoliation of graphite.[36] However, NMP peeled off pentacene/graphene from the SiO_2/Si substrate. Because the surface energy of NMP is similar to that of graphene, NMP has enough energy to remove the pentacene/graphene layers from the SiO_2/Si substrate. In the cases of alcohol and acetone, their surface energies are quite different from that of graphene or pentacene and thus they remove neither pentacene layers nor pentacene/graphene layers from the SiO_2/Si substrate. When the solvents with aromatic or heterocyclic structure (*i.e.*, benzene, toluene, chlorobenzene (CB), and tetrahydrofuran (THF)) were used, only pentacene layers could be removed from the graphene surface. Both benzene and toluene partially removed pentacene layers and 200 nm-thick pentacene islands remained on the graphene surface (Figures 2b and 2c). On the other hand, both CB (Figure 2d) and THF (Figure 2e) effectively removed most of pentacene layers. Although G-THF achieves clean and crack-free graphene, G-CB has pentacene residues on graphene surface and substrate-induced intercalation[4] of CB clusters inside the wrinkles.

In addition, in order to confirm the validity of our transfer method, we fabricated graphene field-effect transistors (FETs) by depositing Au S/D electrodes on top of the transferred graphene, as shown in Figure 2f. We adopted previously reported model[37] for extracting accurate field-effect mobility. The transferred graphene using benzene, toluene, or CB exhibits lower hole mobilities (benzene: 2150 $cm^2/V\cdot s$, toluene: 2680 $cm^2/V\cdot s$, CB: 4300 $cm^2/V\cdot s$) than that using THF (8050 $cm^2/V\cdot s$). The low mobilities in the FETs using benzene or toluene are due to pentacene residues covering graphene surface. These residues can provide scattering sites for charge carriers, thereby interrupting charge transport from source to drain electrode. Meanwhile, FETs based on transferred graphene using CB exhibited positively shifted Dirac voltage (~70 V) and slightly lower mobility than that using THF. In Figure 2d, residues with various sizes (blue arrows) were evident on the graphene basal plane and the big particles (black arrows) were predominantly observed in the graphene wrinkles. We speculate that these big particles are originated from intercalated CB between graphene and target substrate. This explanation is supported by our recent report which used chloroform as a solvent for removing PMMA.[4] Because polar solvents such as CB can be spontaneously intercalated between graphene and target substrate and consequently can dope graphene, the positively shifted Dirac voltage and low mobility were obtained in FETs based on transferred graphene undergoing this solvent treatment. On the other hand, THF treatment fully removed the pentacene layer and there was no discernible intercalation of solvent. In this regard, THF is the best solvent for removing pentacene layer. Accordingly, transferred graphene undergoing THF treatment exhibited excellent electrical properties. The normalized Raman spectrum (inset in Figure 3a) of G-THF also supports doping-free property of G-THF without pentacene residues. Because the D-peak of graphene at 1350 cm^{-1} was not observed, defects were not apparently generated during the transfer process involving a pentacene supporting layer. Uniformity of G-THF was also confirmed by Raman mapping result and distribution of G-peak position (1586 ± 5 cm^{-1}), as shown in Figure 3a. UV–vis spectroscopy measurement was performed to confirm the transmittance of pentacene/graphene film on cover glass before and after chemical removal of pentacene (Figure 3b). The spectra showed that the transmittance (at 550 nm wavelength) of graphene after pentacene removal is ~97.7%, which corresponds to the transmittance of monolayer graphene (2.3%).

For further confirmation of clean surface as well as large-area uniformity of G-THF, we additionally performed millimeter-scale Raman mapping (>2 × 2 mm^2), TEM measurement, and sheet resistance mapping. Raman spectroscopy measurement confirmed

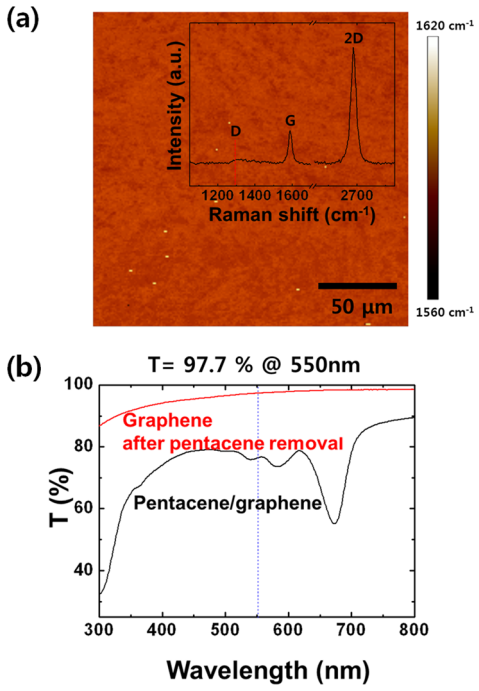

Figure 3. (a) Raman map (position of G-peak) of G-THF (Inset: normalized Raman spectrum). (b) UV–vis spectra of pentacene/graphene and G-THF.

that average Raman spectrum (~10^4 point) of G-THF did not show pentacene peaks ranged from 1158 to 1533 cm^{-1} and position of G-peak was uniformly distributed (Supporting Information, Figure S3). Considering that Raman spectroscope can detect small pentacene residues (height below a few nanometer), it can be concluded that pentacene was totally removed from the surface of graphene. In addition, through TEM measurement, we reaffirmed that G-THF does not generate the pentacene residues whereas G-TR generates the residues (Supporting Information, Figure S4). Electrical uniformity was also evaluated by performing sheet resistance mapping (5 × 5 cm^2). The results showed that average sheet resistance was measured to be 665 ohm/sq (Supporting Information, Figure S5).

We investigated desorption mechanism of pentacene supporting layer from the surface of graphene. Because pentacene cannot be dissolved in THF, the desorption mechanism of pentacene may have involved the intercalation of THF at the interface between the pentacene and graphene. THF may have weakened the $\pi-\pi$ interactions between the pentacene and graphene, thereby inducing spontaneous desorption of the pentacene from the graphene surfaces, as schematically illustrated in Figure 4a. To confirm the validity of the mechanism, pentacene/graphene/SiO_2/Si substrates were immersed into THF and desorption characteristic of pentacene was examined. Pentacene desorbed from the graphene surface maintained a crystal form as confirmed by the observation of the pentacene crystal fragments in FESEM

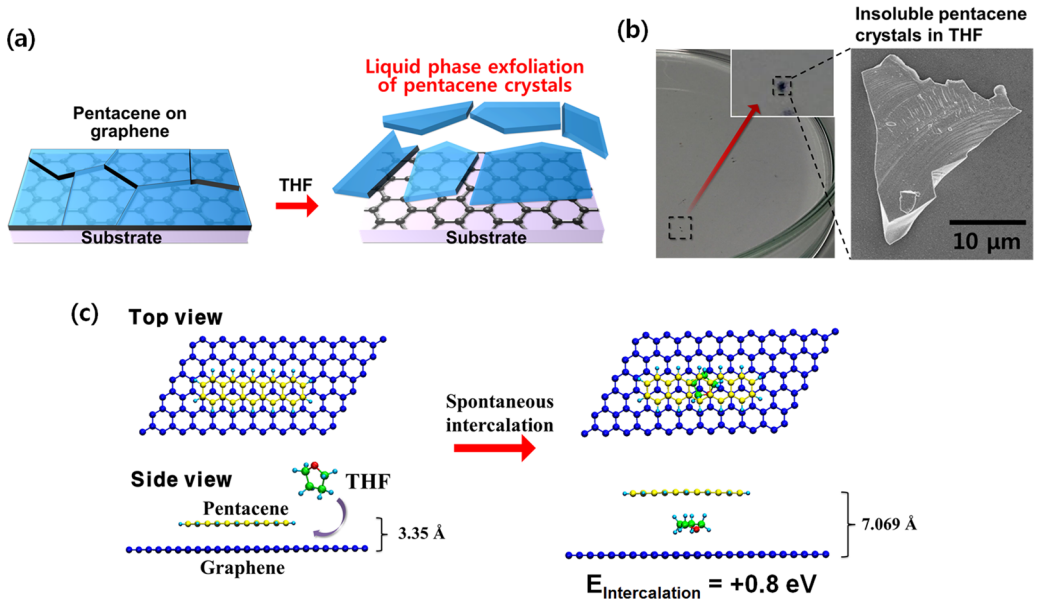

Figure 4. (a) Schematic illustration of the peel-off procedure of pentacene layer from the graphene in THF. (b) Photograph of a Petri dish containing THF after immersing the pentacene/graphene/SiO_2/Si sample and SEM image of a pentacene crystal fragment after removal from the graphene surface. (c) A schematic illustration of spontaneous intercalation of THF between pentacene and graphene interface.

image, as shown in Figure 4b. On the basis of this finding, the solvent-dependent removal of pentacene can also be explained; the molecular asymmetry of solvent can change polarity of solvent, thereby affecting removal characteristics. There was a report that removal of graphite can be dominantly influenced by polarity of solvents.[38] Therefore, we speculate that the degree of pentacene removal from graphene surface is proportional to relative polarity of solvents[39] (benzene: 0.111, toluene: 0.099, CB: 0.188, THF: 0.207).

We additionally performed the theoretical calculation for intercalation energy of THF into pentacene/graphene interface. First we calculated the interaction energy between pentacene molecule and graphene, THF and pentacene molecule, THF and graphene, and THF with neighboring THF. Calculation results showed that the interaction energy for the most stable complex of graphene and pentacene is 1.95 eV at the vertical stacking distance of 3.35 Å with the AB stacking form (Supporting Information, Figure S6). The interaction energy for the most stable complex of THF with graphene or pentacene was calculated to be 0.65 or 0.49 eV and interaction energy between two THF molecules is 0.139 eV (Supporting Information, Figure S7). Using these stable configurations, the intercalation energy of THF into pentacene/graphene was calculated using the equation below:

$$E_{\text{intercalation}} = -(E_{\text{PEN-THF-GR}} - E_{\text{PEN-GR}} - E_{\text{THF}}) \quad (1)$$

where $E_{\text{PEN-THF-GR}}$, $E_{\text{PEN-GR}}$, and E_{THF} is the total energy of pentacene–THF–graphene, pentacene–graphene, and THF–THF system, respectively. The calculation result showed that intercalation energy was calculated to be +0.8 eV (at 0 K, endothermic) at the distance between pentacene and graphene of 7.069 Å, which means that THF can be spontaneously intercalated into pentacene/graphene interface. Therefore, it can be concluded that an intercalated THF molecule between graphene and pentacene would result in the removal of pentacene from the graphene surface, as schematically shown in Figure 4c.

One of the most important advantages of our transfer method using pentacene is that the carrier transport in graphene can be improved because charged impurity scattering caused by residues was minimized. When polar particles on graphene surface are adsorbed on graphene surface, scattering mechanism changes from a short-range scattering (atomic defects in the lattice) to a long-range scattering (charged impurity scattering).[40] Accordingly, charge carrier mobility of graphene is degraded significantly. However, graphene transferred by our method is expected to have homogeneous charge distribution because surface of the graphene (G-THF) is clean without pentacene residues. For the verification of charge homogeneity in graphene, Kelvin probe force microscopy (KPFM) images were obtained, as shown in Figure 5a–c). The KPFM can measure 2-dimensional scan of the relative surface potential difference between tip and substrate.[41] Homogeneous surface potential over large-area was measured in G-THF (Figure 5a), whereas G-TR exhibits high variation in the potential profile (Figure 5b). We speculate that thermal annealing induces strong interaction between graphene and

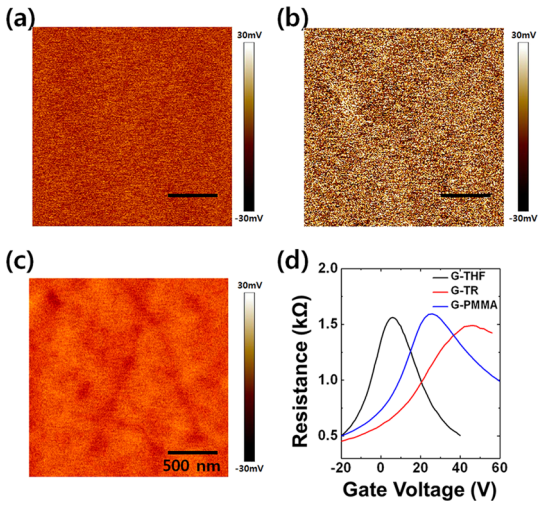

Figure 5. Surface potential maps of (a) G-THF, (b) G-TR, and (c) graphene transferred by conventional wet transfer method using PMMA (G-PMMA). (d) Transfer characteristics of G-TR, G-THF, and G-PMMA.

substrate, thereby increasing charged impurity scattering. On the other hand, graphene transferred by conventional wet transfer method using PMMA (PMMA transfer)[19] exhibits particle-like inhomogeneity (with submicron size) of surface potential in some regions (Figure 5c). We surmise that the origin of this inhomogeneity is directly correlated with PMMA residues. Further work is underway to delineate this inhomogeneous surface potential. The KPFM results show that the surface of G-THF is better than G-TR or G-PMMA with respect to charge transport.

The transfer characteristics of G-THF, G-TR, G-PMMA were compared, as shown in Figure 5d. The V_{Dirac} value of the FET prepared with G-TR was measured to be 48 V. On the other hand, the V_{Dirac} of the FET prepared G-THF was 7 V. This indicated that G-TR displayed p-doping characteristic, whereas doping was negligible in the G-THF. The p-doping characteristics in G-TR were further confirmed by comparing the Raman spectra in Figure 2a. The Raman spectrum of G-TR showed a decrease in I_{2D}/I_G and a blue shift in the G-band compared to that of G-THF. This change in the Raman spectrum was due to the stiffening and sharpening of the G band caused by a breakdown of the adiabatic Born−Oppenheimer approximation and to the channel blocking of phonon decay into the e−h pair.[42,43] Thus, G-TR and G-THF showed different doping characteristics, even though the CVD-grown graphene samples were of identical quality. Thermal annealing has been reported to induce p-doping of graphene by increasing charge transfer between adsorbates on the SiO_2 surface and graphene.[7,26,29] For this reason, G-TR exhibited p-doping characteristics. On the other hand, such effects were minimized when THF was used during graphene transfer. THF was easily removed under vacuum or with mild annealing below 100 °C because THF could be spontaneously intercalated at the interface between pentacene and graphene. Thus, the G-THF displayed undoped characteristics with a minimum shift in the V_{Dirac}.

To find a direct evidence for clean transfer of graphene, we performed XPS measurement of three samples: transferred pentacene (200 nm)/graphene film, G-TR, and G-THF (Supporting Information, Figure S8). In the pentacene/graphene film, 200 nm-thick pentacene layer excepting graphene can only contribute to the observed peak because XPS measurement is a surface-sensitive technique. Although there is a structural similarity between graphene and pentacene, C 1s peak is known to show different position (284.6 eV for graphene on SiO_2,[10] 284.4 eV for pentacene[44]) due to the carrier density difference.[7] Our results showed that C 1s peaks corresponding to sp^2- and sp^3-hybridized states shifted to higher binding energy after removal of pentacene and full width at half-maximum (fwhm) values were reduced from 1.21 eV (pentacene/graphene) to 1.08 eV (G-TR) and 0.987 eV (G-THF), respectively. Accordingly, the narrower C 1s peak at 284.7 eV was observed in G-THF while G-TR exhibited broader peak and the position was shifted to the relatively lower binding energy (284.5 eV). The shift of peak in G-TR might be due to the structural distortion and p-doping of graphene after thermal annealing.[7] Importantly, the broad shoulder peaks ranging from 286 to 290 eV, which are originated from oxidized pentacene (*i.e.*, C−O bond) during transfer process, were commonly observed both in pentacene/graphene and in G-TR, whereas G-THF did not exhibit these shoulder peaks. These results support our claim that thermal annealing could not completely remove pentacene and THF-mediated removal of pentacene enabled graphene transfer without forming a residue.

We then calculated the field-effect mobilities of the GFETs prepared with G-TR or G-THF. Electrical results showed that the hole mobility of G-TR was calculated to be 4300 $cm^2/V \cdot s$. The low field-effect mobility in the FETs prepared with G-TR was due to the presense of residual pentacene particles on the graphene surfaces and/or the p-doping characteristic. Long-range scattering caused by annealing-induced p-doping effects significantly decreased the carrier mobility. Higher hole and electron mobilities were observed in FETs prepared with G-THF: 8050 and 9940 $cm^2/V \cdot s$, respectively. These values were almost two times higher than the field-effect mobilities obtained from the G-PMMA (PMMA-transferred graphene).[5,10] For the accurate comparison, 30 transistors of G-THF and G-PMMA were fabricated using CVD-grown graphene from the same batch. The structure and optical microscopy images of fabricated FETs were shown in Figure S9 and the electrical properties were measured under the same condition. For the fabrication of the devices,

we did not select the specific area of graphene; S/D electrodes were randomly deposited. The channel width and length were 300 and 150 μm, which is long enough to be influenced by microsized cracks in graphene. Compared with G-PMMA, hole and electron mobilities of G-THF were much higher and narrowly distributed, as shown in Figure S10. We surmise that the higher mobility in the FETs prepared with G-THF could be attributed to the undoped graphene characteristics resulting from the clean graphene surface without charged impurities. Any residue present on a graphene surface can increase the charged impurity scattering. G-THF was free of residues, thereby boosting the field-effect mobility of the resulting GFETs. The clean and doping-free transfer method developed here may be used to enhance the electrical responses of graphene-based devices such as ultrasensitive graphene sensors.

CONCLUSION

In conclusion, we developed a new method for transferring large-area CVD-grown graphene onto an arbitrary substrate using a pentacene supporting layer. Our method enables the clean, reproducible, doping-free, and defect-free transfer of graphene. The graphene transferred using pentacene was demonstrated to display enhanced homogeneity in surface potential profiles and electrical properties in the context of an FET after the appropriate removal of pentacene. Liquid phase exfoliation induced removal of pentacene is better than thermal removal process as the former provides doping-free graphene without pentacene residue.

METHODS

Growth of Monolayer Graphene. Copper foil was heated to 1000 °C under H_2 flowing at 20 s.c.c.m. (100 mTorr) for 1 h, followed by flowing 45 s.c.c.m. of CH_4 gas (300 mTorr) for 30 min and rapid cooling of chamber to room temperature under H_2 flowing at 20 s.c.c.m..

Graphene Transfer Using Pentacene. 200 nm-thick pentacene (Aldrich Chemicals, no purification) was deposited onto graphene/copper foil at a rate of 0.5 Å/s by using an organic molecular-beam deposition system under a base pressure of approximately 10^{-7} Torr, followed by etching of the graphene on the back side of the copper foil using oxygen plasma. Pentacene/graphene/copper foil was then floated in an aqueous solution of 0.1 M ammonium persulfate ($(NH_4)_2S_2O_8$). After all of the copper foil was etched away, the graphene film with the pentacene supporting layer was moved to a deionized water for 10 min, and then transferred to a target substrates. The pentacene supporting layer was then removed by conducting thermal annealing at 250 °C or immersing the pentacene/graphene/substrate into tetrahydrofuran (THF).

Characterization. The graphene films were characterized with optical microscopy (Zeiss Axioskop), atomic force microscopy/Kelvin probe force microscopy (AFM/KPFM, Digital Instruments Multimode), field-emission scanning electron microscopy (FESEM, Hitachi S-4800), Raman spectroscopy (Alpha300R, WITec, λ = 532 nm), and UV−vis spectroscopy (Varian, CARY-5000). For characterization of the current−voltage properties of the FET devices, Keithley 4200 semiconductor parameter analyzer was employed.

Methods for Theoretical Calculation. Interaction energy calculations of the systems was performed using the Vienna *Ab-initio* Simulation Package (VASP). For modeling of ion cores, projector augmented wave (PAW) pseudopotentials with 600 eV energy cutoff for the plane wave basis set were used. The exchange-correlation energy was calculated with the generalized gradient approximation (GGA) functional of the Perdew−Burke−Ernzerhof (PBE) type. In addition, the van der Waals density functional theory (vdW-DF) was used to include the dispersion interactions in the system.

Conflict of Interest: The authors declare no competing financial interest.

Acknowledgment. This work was supported by grants from the Basic Science Research Program (2012R1A2A2A04047240) through NRF of Korea and the Center for Advanced Soft Electronics under the Global Frontier Research Program (Code No. 2012M3A6A5055728) of the Ministry of Science, ICT and Future Planning, Korea.

Supporting Information Available: Additional results. This material is available free of charge *via* the Internet at http://pubs.acs.org.

REFERENCES AND NOTES

1. Balandin, A. A. Thermal Properties of Graphene and Nanostructured Carbon Materials. *Nat. Mater.* **2011**, *10*, 569–581.
2. Lee, C.; Wei, X.; Kysar, J. W.; Hone, J. Measurement of the Elastic Properties and Intrinsic Strength of Monolayer Graphene. *Science* **2008**, *321*, 385–388.
3. Blake, P.; Hill, E. W.; Neto, A. H. C.; Novoselov, K. S.; Jiang, D.; Yang, R.; Booth, T. J.; Geim, A. K. Making Graphene Visible. *Appl. Phys. Lett.* **2007**, *91*, 063124–3.
4. Kim, H. H.; Yang, J. W.; Jo, S. B.; Kang, B.; Lee, S. K.; Bong, H.; Lee, G.; Kim, K. S.; Cho, K. Substrate-Induced Solvent Intercalation for Stable Graphene Doping. *ACS Nano* **2013**, *7*, 1155–1162.
5. Lee, W. H.; Park, J.; Kim, Y.; Kim, K. S.; Hong, B. H.; Cho, K. Control of Graphene Field-Effect Transistors by Interfacial Hydrophobic Self-Assembled Monolayers. *Adv. Mater.* **2011**, *23*, 3460–3464.
6. Lee, W. H.; Park, J.; Sim, S. H.; Jo, S. B.; Kim, K. S.; Hong, B. H.; Cho, K. Transparent Flexible Organic Transistors Based on Monolayer Graphene Electrodes on Plastic. *Adv. Mater.* **2011**, *23*, 1752–1756.
7. Lee, W. H.; Park, J.; Sim, S. H.; Lim, S.; Kim, K. S.; Hong, B. H.; Cho, K. Surface-Directed Molecular Assembly of Pentacene on Monolayer Graphene for High-Performance Organic Transistors. *J. Am. Chem. Soc.* **2011**, *133*, 4447–4454.
8. Lim, S.; Kang, B.; Kwak, D.; Lee, W. H.; Lim, J. A.; Cho, K. Inkjet-Printed Reduced Graphene Oxide/Poly(Vinyl Alcohol) Composite Electrodes for Flexible Transparent Organic Field-Effect Transistors. *J. Phys. Chem. C* **2012**, *116*, 7520–7525.
9. Park, J.; Jo, S. B.; Yu, Y. J.; Kim, Y.; Yang, W.; Lee, W. H.; Kim, H. H.; Hong, B. H.; Kim, P.; Cho, K.; *et al.* Single-Gate Bandgap Opening of Bilayer Graphene by Dual Molecular Doping. *Adv. Mater.* **2012**, *24*, 407–411.
10. Park, J.; Lee, W. H.; Huh, S.; Sim, S. H.; Kim, S. B.; Cho, K.; Hong, B. H.; Kim, K. S. Work-Function Engineering of Graphene Electrodes by Self-Assembled Monolayers for High-Performance Organic Field-Effect Transistors. *J. Phys. Chem. Lett.* **2011**, *2*, 841–845.
11. Schwierz, F. Graphene Transistors. *Nat. Nanotechnol.* **2010**, *5*, 487–496.
12. Eda, G.; Lin, Y. Y.; Miller, S.; Chen, C. W.; Su, W. F.; Chhowalla, M. Transparent and Conducting Electrodes for Organic

Electronics from Reduced Graphene Oxide. *Appl. Phys. Lett.* **2008**, *92*, 233305.
13. Lee, S. K.; Kim, B. J.; Jang, H.; Yoon, S. C.; Lee, C.; Hong, B. H.; Rogers, J. A.; Cho, J. H.; Ahn, J. H. Stretchable Graphene Transistors with Printed Dielectrics and Gate Electrodes. *Nano Lett.* **2011**, *11*, 4642–4646.
14. Novoselov, K. S.; Geim, A. K.; Morozov, S. V.; Jiang, D.; Zhang, Y.; Dubonos, S. V.; Grigorieva, I. V.; Firsov, A. A. Electric Field Effect in Atomically Thin Carbon Films. *Science* **2004**, *306*, 666–669.
15. Luo, J.; Kim, J.; Huang, J. Material Processing of Chemically Modified Graphene: Some Challenges and Solutions. *Acc. Chem. Res.* **2013**, *46*, 2225–2234.
16. Kim, J.; Cote, L. J.; Huang, J. X. Two Dimensional Soft Material: New Faces of Graphene Oxide. *Acc. Chem. Res.* **2012**, *45*, 1356–1364.
17. Kim, J. W.; Kang, D.; Kim, T. H.; Lee, S. G.; Byun, N.; Lee, D. W.; Seo, B. H.; Ruoff, R. S.; Shin, H. S. Mosaic-Like Monolayer of Graphene Oxide Sheets Decorated with Tetrabutylammonium Ions. *ACS Nano* **2013**, *7*, 8082–8088.
18. Virojanadara, C.; Syväjarvi, M.; Yakimova, R.; Johansson, L. I.; Zakharov, A. A.; Balasubramanian, T. Homogeneous Large-Area Graphene Layer Growth on 6H-SiC(0001). *Phys. Rev. B: Condens. Matter Mater. Phys.* **2008**, *78*, 245403.
19. Li, X.; Cai, W.; An, J.; Kim, S.; Nah, J.; Yang, D.; Piner, R.; Velamakanni, A.; Jung, I.; Tutuc, E.; *et al.* Large-Area Synthesis of High-Quality and Uniform Graphene Films on Copper Foils. *Science* **2009**, *324*, 1312–1314.
20. Xue, Y. Z.; Wu, B.; Jiang, L.; Guo, Y. L.; Huang, L. P.; Chen, J. Y.; Tan, J. H.; Geng, D. C.; Luo, B. R.; Hu, W. P.; *et al.* Low Temperature Growth of Highly Nitrogen-Doped Single Crystal Graphene Arrays by Chemical Vapor Deposition. *J. Am. Chem. Soc.* **2012**, *134*, 11060–11063.
21. Wu, B.; Geng, D.; Xu, Z.; Guo, Y.; Huang, L.; Xue, Y.; Chen, J.; Yu, G.; Liu, Y. Self-Organized Graphene Crystal Patterns. *NPG Asia Mater.* **2013**, *5*, e36.
22. Wang, D. Y.; Huang, I. S.; Ho, P. H.; Li, S. S.; Yeh, Y. C.; Wang, D. W.; Chen, W. L.; Lee, Y. Y.; Chang, Y. M.; Chen, C. C.; *et al.* Clean-Lifting Transfer of Large-Area Residual-Free Graphene Films. *Adv. Mater.* **2013**, *25*, 4521–4526.
23. Wang, Y.; Zheng, Y.; Xu, X. F.; Dubuisson, E.; Bao, Q. L.; Lu, J.; Loh, K. P. Electrochemical Delamination of CVD-Grown Graphene Film: Toward the Recyclable Use of Copper Catalyst. *ACS Nano* **2011**, *5*, 9927–9933.
24. Batzill, M. The Surface Science of Graphene: Metal Interfaces, CVD Synthesis, Nanoribbons, Chemical Modifications, and Defects. *Surf. Sci. Rep.* **2012**, *67*, 83–115.
25. de Souza, J. M.; Yoshimura, H. N.; Peres, F. M.; Schön, C. G. Effect of Sample Pre-Cracking Method and Notch Geometry in Plane Strain Fracture Toughness Tests as Applied to a PMMA Resin. *Polym. Test.* **2012**, *31*, 834–840.
26. Cheng, Z.; Zhou, Q.; Wang, C.; Li, Q.; Fang, Y. Toward Intrinsic Graphene Surfaces: A Systematic Study on Thermal Annealing and Wet-Chemical Treatment of SiO_2-Supported Graphene Devices. *Nano Lett.* **2011**, *11*, 767–771.
27. Ishigami, M.; Chen, J. H.; Cullen, W. G.; Fuhrer, M. S.; Williams, E. D. Atomic Structure of Graphene on SiO_2. *Nano Lett.* **2007**, *7*, 1643–1648.
28. Suk, J. W.; Lee, W. H.; Lee, J.; Chou, H.; Piner, R. D.; Hao, Y.; Akinwande, D.; Ruoff, R. S. Enhancement of the Electrical Properties of Graphene Grown by Chemical Vapor Deposition *via* Controlling the Effects of Polymer Residue. *Nano Lett.* **2013**, *13*, 1462–1467.
29. Ni, Z. H.; Wang, H. M.; Luo, Z. Q.; Wang, Y. Y.; Yu, T.; Wu, Y. H.; Shen, Z. X. The Effect of Vacuum Annealing on Graphene. *J. Raman Spectrosc.* **2010**, *41*, 479–483.
30. Nourbakhsh, A.; Cantoro, M.; Klekachev, A.; Clemente, F.; Sorée, B.; van der Veen, M. H.; Vosch, T.; Stesmans, A.; Sels, B.; De Gendt, S. Tuning the Fermi Level of SiO_2-Supported Single-Layer Graphene by Thermal Annealing. *J. Phys. Chem. C* **2010**, *114*, 6894–6900.
31. Ryu, S.; Liu, L.; Berciaud, S.; Yu, Y.-J.; Liu, H.; Kim, P.; Flynn, G. W.; Brus, L. E. Atmospheric Oxygen Binding and Hole Doping in Deformed Graphene on a SiO_2 Substrate. *Nano Lett.* **2010**, *10*, 4944–4951.
32. Gao, L. B.; Ni, G. X.; Liu, Y. P.; Liu, B.; Neto, A. H. C.; Loh, K. P. Face-to-Face Transfer of Wafer-Scale Graphene Films. *Nature* **2014**, *505*, 190–194.
33. Jee, H.-g.; Han, J.-H.; Hwang, H.-N.; Kim, B.; Kim, H.-s.; Kim, Y. D.; Hwang, C.-C. Pentacene as Protection Layers of Graphene on SiC Surfaces. *Appl. Phys. Lett.* **2009**, *95*, 093107–3.
34. Fukagawa, H.; Yamane, H.; Kataoka, T.; Kera, S.; Nakamura, M.; Kudo, K.; Ueno, N. Origin of the Highest Occupied Band Position in Pentacene Films from Ultraviolet Photoelectron Spectroscopy: Hole Stabilization *versus* Band Dispersion. *Phys. Rev. B: Condens. Matter Mater. Phys.* **2006**, *73*, 245310.
35. Seto, K.; Furukawa, Y. Study on Solid Structure of Pentacene Thin Films Using Raman Imaging. *J. Raman Spectrosc.* **2012**, *43*, 2015–2019.
36. Hernandez, Y.; Nicolosi, V.; Lotya, M.; Blighe, F. M.; Sun, Z.; De, S.; McGovern, I. T.; Holland, B.; Byrne, M.; Gun'Ko, Y. K.; *et al* High-Yield Production of Graphene by Liquid-Phase Exfoliation of Graphite. *Nat. Nanotechnol.* **2008**, *3*, 563–568.
37. Kim, S.; Nah, J.; Jo, I.; Shahrjerdi, D.; Colombo, L.; Yao, Z.; Tutuc, E.; Banerjee, S. K. Realization of a High Mobility Dual-Gated Graphene Field-Effect Transistor with Al_2O_3 Dielectric. *Appl. Phys. Lett.* **2009**, *94*, 062107.
38. Schlierf, A.; Yang, H. F.; Gebremedhn, E.; Treossi, E.; Ortolani, L.; Chen, L. P.; Minoia, A.; Morandi, V.; Samori, P.; Casiraghi, C.; *et al.* Nanoscale Insight into the Exfoliation Mechanism of Graphene with Organic Dyes: Effect of Charge, Dipole and Molecular Structure. *Nanoscale* **2013**, *5*, 4205–4216.
39. Reichardt, C. *Solvents and Solvent E□ects in Organic Chemistry*, 3rd ed.; Wiley-VCH: Weinheim, 2003.
40. Chen, J. H.; Jang, C.; Adam, S.; Fuhrer, M. S.; Williams, E. D.; Ishigami, M. Charged-Impurity Scattering in Graphene. *Nat. Phys.* **2008**, *4*, 377–381.
41. Zhou, X.; He, S.; Brown, K. A.; Mendez-Arroyo, J.; Boey, F.; Mirkin, C. A. Locally Altering the Electronic Properties of Graphene by Nanoscopically Doping It with Rhodamine 6G. *Nano Lett.* **2013**, *13*, 1616–1621.
42. Das, A.; Pisana, S.; Chakraborty, B.; Piscanec, S.; Saha, S. K.; Waghmare, U. V.; Novoselov, K. S.; Krishnamurthy, H. R.; Geim, A. K.; Ferrari, A. C.; *et al.* Monitoring Dopants by Raman Scattering in an Electrochemically Top-Gated Graphene Transistor. *Nat. Nanotechnol.* **2008**, *3*, 210–215.
43. Pisana, S.; Lazzeri, M.; Casiraghi, C.; Novoselov, K. S.; Geim, A. K.; Ferrari, A. C.; Mauri, F. Breakdown of the Adiabatic Born−Oppenheimer Approximation in Graphene. *Nat. Mater.* **2007**, *6*, 198–201.
44. Kang, S. J.; Kim, C. Y.; Cho, S. W.; Noh, M.; Jeong, K.; Whang, C. N. Energy Level Diagrams of C_{60}/Pentacene/Au and Pentacene/C_{60}/Au. *Synth. Met.* **2006**, *156*, 32–37.